

## 9. Adaptive ENO-Wavelet Transforms for Discontinuous Functions

T.F. Chan<sup>1</sup> H.M. Zhou<sup>2</sup>

### Introduction

We have designed an adaptive ENO-wavelet transform for approximating discontinuous functions without oscillations near the discontinuities. Our approach is to apply the one-side information idea from Essentially Non-Oscillatory (ENO) schemes for numerical shock capturing to standard wavelet transforms. This transform retains the essential properties and advantages of standard wavelet transforms such as concentrating the energy to the low frequencies and having a multiresolution framework and fast algorithms, all without any edge artifacts. Furthermore, we have obtained a rigorous uniform approximation error bound regardless of the presence of discontinuities. We will show some numerical examples and some applications to image compression.

It is well known that wavelet linear approximation (i.e. truncating the high frequencies) can approximate smooth functions very efficiently but cannot achieve similar results for piecewise continuous functions, especially functions with large jumps. Several problems arise near jumps, primarily caused by the well-known Gibb's phenomenon. The jumps generate large high frequency wavelet coefficients and thus linear approximations cannot get the same high accuracy near discontinuities as in the smooth region.

To overcome these problems within the standard wavelet transform framework, non-linear data-dependent approximations, which selectively retain certain high frequency coefficients, are often used, e.g. hard and soft thresholding techniques, see [Don95],[Mal98]. Another way is to construct orthonormal basis to represent the discontinuities, such as Donoho's wedgelets [Don97], rigdelets [CD99b], and curvelets [CD99a], and Mallat's bandelets [Mal00].

A different approach is to modify the wavelet transform to not generate large wavelet coefficients near jumps. Claypoole, Davis, Sweldens and Baraniuk [PCB99] proposed an adaptive lifting scheme which lowers the order of approximation near jumps, thus minimizing the Gibbs' effect. We use a different approach in developing our ENO-wavelet transforms by borrowing the well developed Essentially Non-Oscillatory (ENO) technique for shock capturing in computational fluid dynamics (e.g. see [AHC87]) to modify the standard wavelet transform near discontinuities so that the Gibbs' phenomenon can be completely removed. ENO schemes are systematic ways of adaptively defining piecewise polynomial approximations of the given functions according to their smoothness. A crucial point in designing ENO schemes is to use one-sided information near jumps, and never differencing across the discontinuities.

Combining the ENO idea with the multiresolution data representation is a natural

---

<sup>1</sup>Department of Mathematics, UCLA, chan@ipam.ulca.edu. Research supported in part by grants ONR-N00017-96-1-0277 and NSF DMS-9973341. The material in this report is patent pending.

<sup>2</sup>Department of Applied Mathematics, Caltech, hmzhou@acm.caltech.edu

way to avoid oscillations in the approximations. In fact, it has been explored by Harten in his general framework of multiresolution [Har94], which is similar to the lifting scheme of Sweldens [Swe97]. However, his method was not developed to be directly applied to the widely used pyramidal filtering algorithms which the standard wavelet transforms are usually implemented in.

The way we accomplish this is to not change the wavelet transforms or the filter coefficients, which most data dependent multiresolution algorithms do, but instead locally change the function near the discontinuities in such a way that the standard filters are only applied to smooth data, and therefore no large high frequency coefficients are generated. By recording how the changes are made, the original discontinuous function can be exactly recovered by using the original inverse filters. We show that the resulting wavelet transform retains all the desirable properties of the standard transform. The extra cost (in floating point operations) required is insignificant, which, in fact, is of order  $O(dl)$  where  $d$  is the number of discontinuities and  $l$  the filter length.

The arrangement of the paper is as follows. In the next section, we give a general algorithm to implement the ENO-wavelet transform discretely. And we also state the rigorous uniform error estimate in this section. In the last section, we give some numerical examples to illustrate the main advantage of the ENO-wavelet transforms, including some examples in image compression.

In this short proceeding paper, we are forced to leave out many mathematical details, and we aim only to give a general idea of the algorithms and the numerical results. For more details, see [CZ99].

## ENO-wavelet Transforms

First, we briefly review the standard discrete wavelet transforms, e.g. see [Dau92], [Mal98] and [SN96]. In practice, discrete wavelet transforms are often used by starting with a set of discrete numbers which are the low frequency coefficients of the  $L^2$  function  $f(x)$  at the finest level. In many applications, this set of numbers are sample values of the function  $f(x)$  on a fine grid (although in [SN96], this is called a "wavelet crime"). Let  $\alpha_{j,k}$  ( $\beta_{j,k}$ ) denote the low (high) frequency coefficients at level  $j$ . The wavelet transform coefficients at a coarser level  $j-1$  can be computed by:

$$\alpha_{j-1,k} = \sum_{s=0}^l c_s \alpha_{j,2k+s}; \quad \beta_{j-1,k} = \sum_{s=0}^l h_s \alpha_{j,2k+s}, \quad (1)$$

where  $c_s$  ( $h_s$ ) are called low (high) pass filters. It is well known that the inverse transforms can be easily formed by using orthogonality of the wavelet transforms. The linear approximation refers to reconstructing  $\alpha_{j,k}$  by setting the high frequencies  $\beta_{j-1,k}$  to zero.

In Fig 1, the left picture is a piecewise continuous function (dotted) and its linear approximation (solid). The middle one is a zoom-in at a discontinuity. We clearly see oscillations near discontinuities. The right one is its DB-4 wavelet coefficients. We see that most of the high frequency coefficients are zero, except for a few large coefficients which these coefficients are computed near jumps. In this figure, we clearly see oscillations near discontinuities.

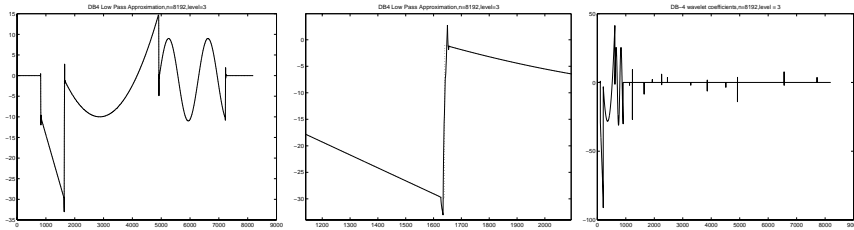


Figure 1: Left: The initial discontinuous function (dotted) and its linear approximation (solid). Middle: A zoom-in at a discontinuity. Oscillations are generated near the discontinuity. Right: its DB4 coefficients. Most of the high frequency coefficients (right part) are zero except for a few large coefficients computed near the jumps.

To simplify the presentation, we shall assume that the discontinuities in the functions are well-separated in the following sense:

**Definition 1** For a given wavelet filter with stencil length  $l$ , we say the  $j$ -th level approximation of the function  $f(x)$  with spatial step  $\Delta x = 2^{-j}$  satisfies the **Discontinuity Separation Property (DSP)** if  $(l + 2)\Delta x < t$ , where  $f(x)$  has discontinuous set  $D$  and  $t$  is the closest distance between any two discontinuous points.

For any piecewise discontinuous function and a fixed stencil length  $l$ , an approximation will satisfy this DSP if  $j$  is sufficiently large, i.e. if the discretization is fine enough. On the other hand, at the place where the DSP is invalid, we will see that the approximations produced by the ENO-wavelet transforms are comparable to that by the standard wavelet transforms.

Now, we are ready to introduce the ENO-wavelet transforms. In addition to the standard wavelet transform computation, ENO-wavelet transforms have two more phases: locating the jumps and forming the approximations at the discontinuities. First, assuming knowledge of the location of the jumps, we give the ENO-wavelet approximations at the discontinuities by using one-sided information to avoid oscillations. Then, we give the methods to detect the location of the discontinuities. We also give the approximation error bound at the end of this section. In this short paper, we only consider Daubechies' orthonormal wavelets. The idea can be similarly extended to other wavelets.

The main idea of the ENO schemes for shock capturing is to use one-sided polynomial interpolations for data with large discontinuities. For ENO wavelets, we borrow this idea of using one-sided information to form the approximation and avoid applying the wavelet filters crossing the discontinuities.

The first way is to directly extend the function values, or in general the low frequencies on the finer level, at the discontinuity by  $p$ -th order extrapolation from both sides. For example, a straightforward way is to use  $p$ -point polynomial extrapolation. Least square can be used too [WA95]. Then one can apply the standard wavelet transforms on the extended functions by using (1) to compute the coarser level wavelet coefficients.

There is a storage problem for this direct function extrapolation. Indeed, it doubles the number of the wavelet coefficients near every discontinuity. To retain the perfect

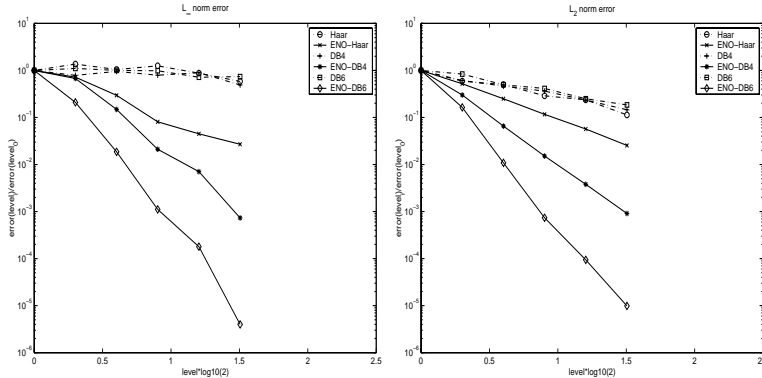


Figure 2: The approximation accuracy comparison of ENO-wavelet and standard wavelet transforms. Both  $L_\infty$  (left) and  $L_2$  (right) order of accuracy show that ENO transforms maintain the order 1, 2 and 3 for ENO-Haar, ENO-DB4 and ENO-DB6 respectively and they agree with the theoretical results. In contrast, standard transforms do not retain the order.

invertible property, we need to store the ENO-wavelet coefficients from both sides. Thus, the output sequences are no longer the same size as the input sequences. In many applications, such as image compression, this extra storage requirement definitely needs to be avoided.

To keep the size of the output sequences the same as that of the input sequences without significant extra computation, we introduce the coarse level extrapolation schemes. The idea is to extrapolate the coarser level wavelet coefficients near the discontinuities instead of the function values or the finer level wavelet coefficients. Let us consider the extension from the left side first.

We have two choices: (1) We can extrapolate the low frequency coefficients  $\alpha_{j-1,k}$  first, then determine the corresponding high frequency coefficients  $\beta_{j-1,k}$ . (2) Or we can first extend high frequency coefficients  $\beta_{j-1,k}$ , for example to zero, then determine the corresponding low frequency coefficients  $\alpha_{j-1,k}$ . By symmetry, we have two analogous choices for the right side of the jump.

The storage problem can be easily solved in both options. For example, we can store the high frequency coefficients for choice (1) and the low frequency coefficients for choice (2). The corresponding low frequency and high frequency coefficients can be easily recovered.

For each stencil crossing a jump, an extra cost (in floating point operation) is required in extrapolating low frequency coefficients, and in computing the corresponding high or low frequency coefficients. Overall, the extra cost over the standard wavelet transform is of order  $O(dl)$ . Compared to the cost of the standard transform, which is of order  $O(nl)$  where  $n$  is the size of data, the ratio of the extra cost over that of the standard transform is  $O(\frac{d}{n})$ , which is independent of  $l$  and negligible when  $n$  is large.

Next, we introduce the methods to detect the location of the discontinuities for noisy and noise free functions. First we consider noise free data.

It is well known that for the smooth functions, we have  $|\beta_{j,i}| = |f^{(p)}|O(\Delta x^p)$ . In

contrast,  $|\beta_{j,i}|$  is at least one order lower than that if it involves a discontinuity. So, an obvious way, also the cheapest way, to identify the discontinuities is to compare the magnitudes of the high frequency coefficients on the current standard stencils  $|\beta_{j,i}|$  with that on the previous standard stencils  $|\beta_{j,i-1}|$ . Thus, we can design a method to detect the discontinuities as follows: If we have  $|\beta_{j,i}| \leq a|\beta_{j,i-1}|$ , where  $a > 1$  is a given thresholding constant, then we treat the current stencil as a smooth stencil. Otherwise, we conclude that there are discontinuities contained in it.

The above described detection method may not be reliable if the function is polluted by noise, especially when the noise is "large". In this situation, we need to use heuristics to locate the exact position of the essential discontinuities. In many applications such as in image processing, large discontinuities in function value are the most significant features. A simple way to detect this kind of discontinuities is to look for these large magnitude high frequency coefficients and then compare the data values in the corresponding stencils to locate the exact jump positions.

Finally, we present the following uniform error estimate; the proof can be found in [CZ99]

**Theorem 1** *Suppose the wavelets have finite support in  $[0, l]$ , and  $p$  vanishing moments,  $f(x)$  is a piecewise continuous function in  $[a, b]$ , and  $f_j(x)$  is its  $j$ -th level ENO-wavelet approximation. If the approximation  $f_{j+1}(x)$  satisfies the DSP, then*

$$\|f(x) - f_j(x)\| \leq C(\Delta x)^p \|f^{(p)}(x)\|_{(a,b) \setminus D}, \tag{2}$$

where  $\Delta x = 2^{-j}$  and  $D$  is the jump set. The norm  $\|\cdot\|$  can be either  $L^2$  or  $L^\infty$ .

This theorem shows that the error in the ENO-wavelet approximation depends only on the size of the derivative of the function away from the discontinuities. In contrast, the error estimate for standard wavelet transforms depends on  $\|f^{(p)}(x)\|_{(a,b)}$  which is unbounded at discontinuities. From an approximation point of view, the error bound for ENO-wavelets is as if the discontinuities were not there, and this is the best possible for discontinuous functions.

## Numerical Examples

In this section, we give some 1-D and 2-D numerical examples by using the ENO-wavelet transforms. In particular, we show results for the ENO-Haar, ENO-DB4 and ENO-DB6 wavelet transforms.

To illustrate the performance of ENO-wavelet transforms, we show picture comparisons of the standard wavelet approximations (dash dotted in all figures) and corresponding ENO-wavelet approximations (solid). In addition, we compare their  $L_\infty$  and  $L_2$  errors at level  $i$ :  $E_{\infty,i}$  and  $E_{2,i}$ . Also, we compute the order of accuracy defined by:  $Order_\infty = \log_2 \frac{E_{\infty,i}}{E_{\infty,i-1}}$ ,  $Order_2 = \log_2 \frac{E_{2,i}}{E_{2,i-1}}$ .

We apply Haar and ENO-Haar, DB4 and ENO-DB4, and DB6 and ENO-DB6 to this function and compare the approximation errors. Fig 2 shows the comparison of the order in  $L_\infty$  and in  $L_2$  norm. It is clear that both the  $L_\infty$  and  $L_2$  order of accuracy for ENO-wavelet transforms are of the order 1, 2 and 3 for ENO-Haar, ENO-DB4 and

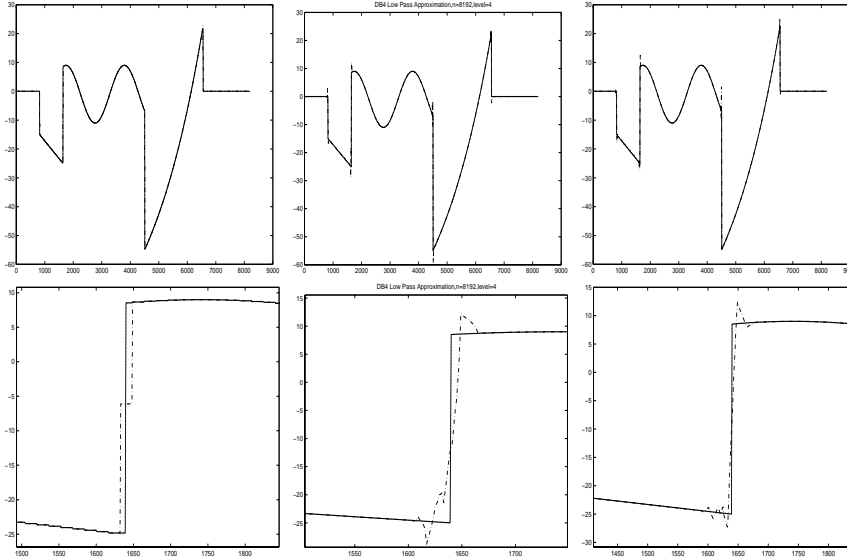


Figure 3: The 4-level ENO-Haar and Haar (left), ENO-DB4 and DB4 (middle), and ENO-DB6 and DB6 (right) approximation. The second row are corresponding zoom-ins near a discontinuity. We see the Gibbs' phenomenon in the standard approximation but not in the ENO approximation.

ENO-DB6 respectively, agreeing with the results of Theorem 1. In contrast, standard wavelet transforms do not retain the corresponding order.

To see the Gibbs' oscillations, we display the 4-level ENO-wavelet and standard wavelet approximations in the first row of Fig 3, for ENO-Haar (left), ENO-DB4 (middle) and ENO-DB6 (right) respectively. The second row are corresponding zoom-in at a same discontinuity. We clearly see the Gibbs' oscillations in the standard approximations. In contrast, the ENO-wavelet approximations preserve the jumps accurately.

In Fig 4, we also present the standard DB4 (dotted) and the ENO-DB4 (solid) wavelet coefficients respectively. There are some large standard high frequency coefficients (right part) related to the discontinuities. On the other hand, no large high frequency coefficients present in the ENO-wavelet coefficients.

The next 1-D example shows the ENO-DB6 wavelet transform applied to noisy data (see Fig. 5). Despite the presence of noise in the initial data (circles), the level-3 ENO-DB6 approximation (solid line) still retains the sharp edges (see zoom-in in the right picture) compared to the standard DB6 approximation (dash-dotted line) which not only has oscillations at the discontinuities but also smears them.

Finally, we give a 2-D image compression example to compare the standard Haar and the ENO-Haar approximations. Here we use tensor products of 1-D transforms. The original picture (left), the 3-level standard Haar (middle) and ENO-Haar (right) approximation are shown in Fig 6. Both approximations use the same number of low frequencies ( $\frac{1}{64}$  of the original data). It is clear that in the standard Haar case, the

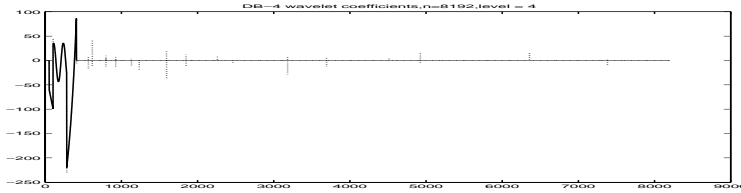


Figure 4: The 4-level ENO-DB4 (solid) and the standard DB4 (dotted) coefficients. There are large high frequency coefficients (right part) near the discontinuities in the standard transform but not in the ENO-DB4 transform.

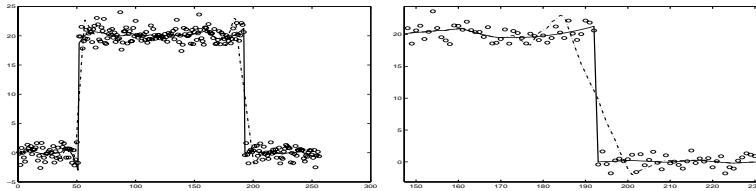


Figure 5: Left: The comparison of the 3-level ENO-DB6 (solid line) with the standard DB6 (dash-dotted line) approximation for noisy initial data (circles). Right: A zoom-in of the left example at a discontinuities. The ENO-DB6 approximation retains the sharp jumps but the standard DB6 approximation does not.

image becomes fuzzier than the ENO-Haar case. This illustrates that the ENO-Haar approximation can reduce the edge oscillations for 2-D images.

## References

[AHC87]S. Osher A. Harten, B. Engquist and S. Chakravarthy. Uniformly high order essentially non-oscillatory schemes, iii. *Journal of Computational Physics*, 71:231–303, 1987.  
 [CD99a]E. Candes and D. Donoho. Curvelets: A surprisingly effective nonadaptive

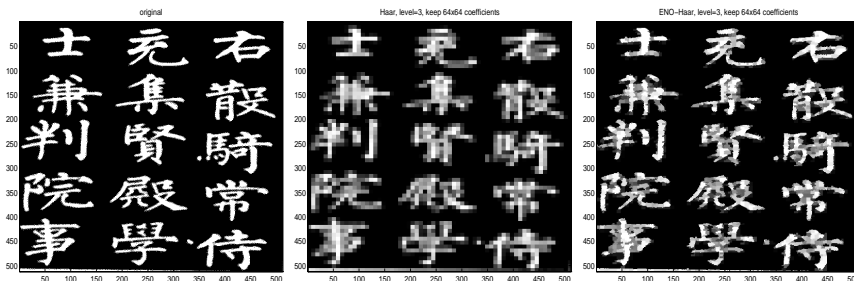


Figure 6: Original 2-d Function (left), The 3-level standard Haar (middle), and the 3-level ENO-Haar (right).

- representation of objects with edges. Technical report, Department of Statistics, Stanford University, 1999.
- [CD99b]E. Candes and D. Donoho. Ridgelets: a key to higher-dimensional intermittency? *Phil. Trans. R. Soc. Lond., A*, 1999.
- [CZ99]T. F. Chan and H. M. Zhou. Adaptive eno-wavelet transforms for discontinuous functions. Technical Report 99-21, Dept. of Math, UCLA, CAM Report,, June 1999.
- [Dau92]I. Daubechies. *Ten Lectures on Wavelets*. SIAM, 1992.
- [Don95]D. Donoho. De-noising by soft thresholding. *IEEE Trans. Inf. Th.*, 41:613–627, 1995.
- [Don97]D. Donoho. Wedgelets: Nearly-minimax estimation of edges. Technical report, Tech Report, Dept. of Stat., Stanford Univ., 1997.
- [Har94]A. Harten. Multiresolution representation of data, ii. general framework. Technical Report 94-10, Dept. of Math., UCLA., CAM Report, April 1994.
- [Mal98]S. Mallat. *A Wavelet Tour of Signal Processing*. Academic Press, 1998.
- [Mal00]S. Mallat. Geometrical image representations with bandelets. The talk at the IMA Workshop on Image Processing and Low Level Vision, held at Minneapolis, Minnesota, Oct 16-20, 2000, Oct. 2000.
- [PCB99]W. Sweldens P. Claypoole, G. Davis and R. Baraniuk. Nonlinear wavelet transforms for image coding. Submitt to IEEE Tran. on Image Proc., 1999.
- [SN96]G. Strang and T. Nguyen. *Wavelets and Filter Banks*. Wellesley-Cambridge Press, 1996.
- [Swe97]W. Sweldens. The lifting scheme: A construction of second generation wavelets. *SIAM J. Math. Anal.*, 29(2):511–546, 1997.
- [WA95]J. R. Williams and K. Amaratunga. A discrete wavelet transform without edge effects. Technical report, MIT, IESL Tech. Report, 1995.